

Modeling and synthesis of a robust autopilot for a cargo ship

RASOAMANANA R. A.¹, RANDRIAMITANTSOA P. A.², RANDRIAMITANTSOA A. A.³

Doctoral School in Sciences and Techniques of Engineering and Innovation
Telecommunications, Automation, Signal and Images Research Laboratory
University of Antananarivo
BP 1500, Ankatso – Antananarivo 101- Madagascar

ABSTRACT

This article uses a nonlinear extension of Nomoto model for ship modeling. Our goal is to synthesize a robust control law for the autopiloting of a cargo ship. A backstepping technique with approximation of the nonlinear function by artificial neural networks is used.

Keywords: Autopilot, ship, robust control, Backstepping, neural network

1. Introduction

Nowadays, the need of an automatic control or autopiloting is useful. So, we will contribute to the synthesis of a robust control law for the autopiloting of a cargo ship in maneuver. A nonlinear extension of the first-order Nomoto model is chosen for its simplicity and fidelity to the actual behavior of the cargo ship. Many simulations of a course-keeping and turning maneuver of the cargo ship will be presented in this article.

2. Cargo ship

A **cargo ship** or **freighter** [1] is a merchant ship whose role is to transport goods in various forms using the seaway.

Cargo ships can be classified according to the type of goods they carry, and how they are transported. The main distinction is made between :

- a « dry » cargo
- a « liquid » cargo

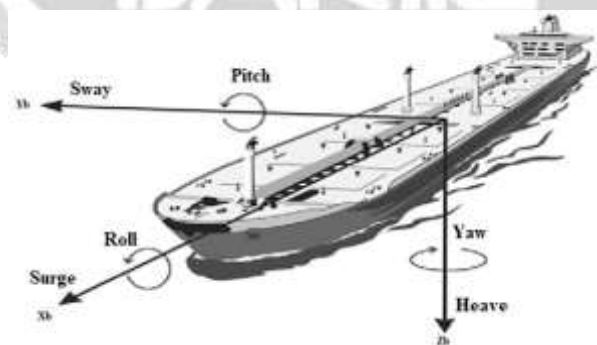


Figure 1 : Degrees of freedom of a ship

Like all conventional ships, cargo ships or freighters have 6 degrees of freedom which are: **surge**, **sway**, **heave**, **roll**, **pitch** and **yaw**. The 6 degrees of freedom of a ship are expressed in **Figure 1**.

Remark 1 :

In this article, we will mainly focus on autopilot, that is, controlling the yaw angle.

3. Autopilot model of Nomoto [2]

3.1. Second order Nomoto model

The linear autopilot model with constant speed u_0 is defined by:

$$M\dot{v} + N(u_0)v = b\delta \quad (1)$$

with $v = [v, r]^T$ is the state vector.

δ is the rudder angle.

$b = \begin{bmatrix} -Y_\delta \\ -N_\delta \end{bmatrix}$ is a hydrodynamic coefficient matrix.

$M = \begin{bmatrix} m - Y_{\dot{v}} & mx_g - Y_{\dot{r}} \\ mx_g - N_{\dot{v}} & I_z - N_{\dot{r}} \end{bmatrix}$ is the inertia matrix.

$N(u_0) = \begin{bmatrix} -Y_v & mu_0 - Y_r \\ -N_v & mx_g u_0 - N_r \end{bmatrix}$ is sum of the Coriolis centripetal term and linear damping.

The yaw rate r is chosen as output such that:

$$\dot{\psi} = r \quad (2)$$

$$r = c^T v, \quad c^T = [0, 1] \quad (3)$$

The Laplace transform of equation (1) gives:

$$\frac{r}{\delta}(s) = \frac{K(1 + T_3 s)}{(1 + T_1 s)(1 + T_2 s)} \quad (4)$$

The time domain representation of the second order model gives:

$$T_1 T_2 \psi^{(3)} + (T_1 + T_2) \ddot{\psi} + \dot{\psi} = K(\delta + T_3 \dot{\delta}) \quad (5)$$

By combining equation (2) and (5), we have:

$$T_1 T_2 \dot{r} + (T_1 + T_2) \dot{r} + r = K(\delta + T_3 \dot{\delta}) \quad (6)$$

3.2. First order Nomoto model

The first order Nomoto model is obtained by calculating the equivalent time constant by:

$$T = T_1 + T_2 - T_3 \quad (7)$$

Such as

$$\frac{r}{\delta}(s) = \frac{K}{(1 + Ts)} \quad (8)$$

The time domain representation of the first order Nomoto model gives:

$$T\ddot{\psi} + \dot{\psi} = K\delta \quad (9)$$

By combining equation (2) and (9), we have:

$$T\dot{r} + r = K\delta \quad (10)$$

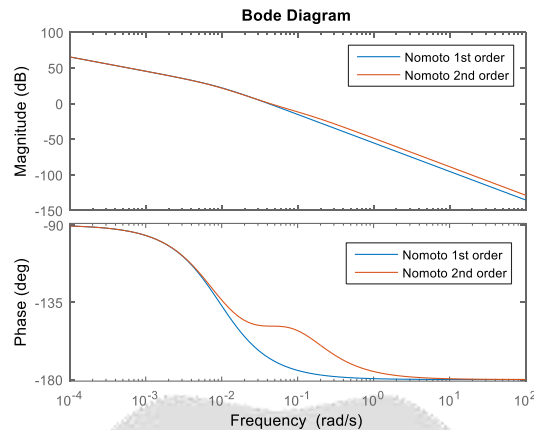


Figure 2 : Frequency response of a cargo ship

The frequency response is shown in **Figure 2**. It shows us that Nomoto first-order autopilot model of a cargo ship is quite accurate at very low frequencies. The difference between the first order and second order model is around the frequency 0.1 rad/s. This is due to the cancellation of the sway dynamics. The first-order model is therefore widely used for modeling a maneuvering cargo ship working at very low frequencies.

3.3. Nonlinear extension of the Nomoto model

The linear Nomoto model can be extended to include nonlinear effects by adding a static nonlinearity describing the maneuver characteristics.

3.3.1. Nonlinear extension of the first order Nomoto model

In [3], the following first order model is proposed :

$$T\dot{r} + H_n(r) = K\delta \tag{11}$$

with

$$H_n(r) = n_3r^3 + n_2r^2 + n_1r + n_0 \tag{12}$$

The equivalent linear model defined by equation (10) is obtained for $H_n(r) = r$.

3.3.2. Nonlinear extension of the second order Nomoto model

In [4], a nonlinear extension of the second order model is proposed :

$$T_1T_2\ddot{r} + (T_1 + T_2)\dot{r} + H_B(r) = K(\delta + T_3\dot{\delta}) \tag{13}$$

with

$$H_B(r) = b_3r^3 + b_2r^2 + b_1r + b_0 \tag{14}$$

The equivalent linear model defined by equation (6) is obtained for $H_B(r) = r$.

4. Autopilot synthesis [5][6][7]

The autopiloting block diagram is given in **Figure 3** below:

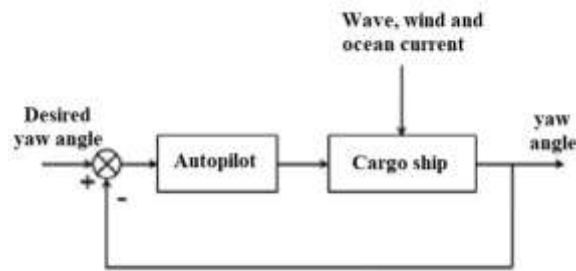


Figure 3 : Autopiloting of a cargo ship

4.1. Nominal backstepping control

Consider the following nonlinear first order nominal model:

$$\dot{\psi} = r \tag{15}$$

$$T\dot{r} + H_N(r) = K\delta \tag{16}$$

In the strict feedback form, we have:

$$\dot{\psi} = r \tag{17}$$

$$\dot{r} = \frac{1}{T}[K\delta - H_N(r)] \tag{18}$$

Autopiloting consists of following the desired yaw angle ψ_d by the yaw angle ψ .

Step 1 : We define the error variable $e_1 = \psi - \psi_d$. Its derivative gives:

$$\dot{e}_1 = \dot{\psi} - \dot{\psi}_d = r - \dot{\psi}_d \tag{19}$$

Consider the following Lyapunov control function:

$$V_1 = \frac{1}{2}e_1^2 \tag{20}$$

Its derivative then gives:

$$\dot{V}_1 = e_1\dot{e}_1 \tag{21}$$

So

$$\dot{V}_1 = e_1(r - \dot{\psi}_d) \tag{22}$$

To ensure the convergence of e_1 , the derivative of the Lyapunov control function must be defined negative therefore,

$$r - \dot{\psi}_d = -k_1e_1 \tag{23}$$

So,

$$r_d = -k_1e_1 + \dot{\psi}_d \tag{24}$$

And

$$\dot{V}_1 = -k_1e_1^2 \tag{25}$$

Step 2 : We define the error variable $e_2 = r - r_d$. Its derivative gives:

$$\dot{e}_2 = \dot{r} - \dot{r}_d = -\frac{H_N(r)}{T} + \frac{K}{T}\delta - \dot{r}_d \tag{26}$$

The nonlinear function $-\frac{H_N(r)}{T}$ composing the model is sometimes difficult to implement in practice. With its approximation by an artificial neural network $\theta^T \xi(r)$, equation (26) gives:

$$\dot{e}_2 = \theta^T \xi(r) + \frac{K}{T}\delta - \dot{r}_d \tag{27}$$

Consider the following Lyapunov control function:

$$V_2 = V_1 + \frac{1}{2} e_2^2 \quad (28)$$

Its derivative gives:

$$\dot{V}_2 = -k_1 e_1^2 + e_2 \dot{e}_2 \quad (29)$$

So

$$\dot{V}_2 = -k_1 e_1^2 + e_2 (\theta^T \xi(r) + \frac{K}{T} \delta - \dot{r}_d) \quad (30)$$

To ensure the convergence of e_2 , the derivative of the Lyapunov control function must be defined negative therefore,

$$\theta^T \xi(r) + \frac{K}{T} \delta - \dot{r}_d = -k_2 e_2 \quad (31)$$

So, the nominal rudder angle control law is given by :

$$\delta = \frac{T}{K} [-\theta^T \xi(r) + \dot{r}_d - k_2 e_2] \quad (32)$$

4.2. « Efficient » nominal backstepping control

To increase the performance of the system [8], we will use the term $\tanh(\cdot)$ defined by the **figure 4**.

Step 1 : Equation (23) then becomes :

$$r - \dot{\psi}_d = -k_1 e_1 - \beta_1 \tanh(\alpha_1 e_1) \quad (33)$$

with $\beta_1 > 0$ et $\alpha_1 > 0$

So,

$$r_d = -k_1 e_1 + \dot{\psi}_d - \beta_1 \tanh(\alpha_1 e_1) \quad (34)$$

And

$$\dot{V}_1 = -k_1 e_1^2 - \beta_1 e_1 \tanh(\alpha_1 e_1) < 0 \quad (35)$$

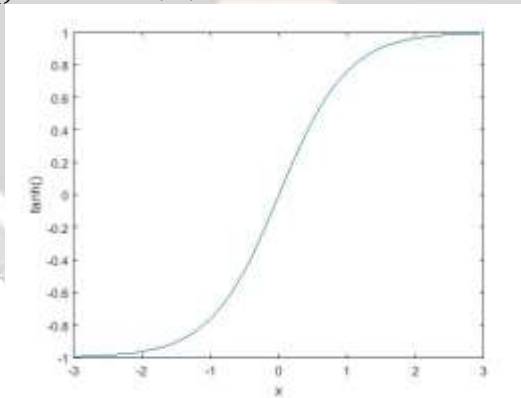


Figure 4 : Hyperbolic tangent function

Etape 2 : Equation (31) then becomes :

$$\theta^T \xi(r) + \frac{K}{T} \delta - \dot{r}_d = -k_2 e_2 - \beta_2 \tanh(\alpha_2 e_2) \quad (36)$$

So, the « efficient » nominal rudder angle control law is given by:

$$\delta = \alpha_1 = \frac{T}{K} [-\theta^T \xi(r) + \dot{r}_d - k_2 e_2 - \beta_2 \tanh(\alpha_2 e_2)] \quad (37)$$

Remark 2 :

The « efficient » backstepping control allows us to :

- increase the performance of the nominal system
- guarantee global asymptotic stability in the case of a system with a bounded or constant external disturbance

4.3. Robust backstepping control

Consider the following first order nonlinear perturbed Nomoto model :

$$\dot{\psi} = r \quad (38)$$

$$T\dot{r} + H_N(r) = K\delta + w\Delta \quad (39)$$

with $w\Delta$ is the external disturbance representing the wind, the wave and the sea current where

- w is a known nonlinear function
- Δ is an uncertain nonlinear term but bounded by Δ_0

In the strict feedback form, we have:

$$\dot{\psi} = r \quad (40)$$

$$\dot{r} = \frac{1}{T} [K\delta + w\Delta - H_N(r)] \quad (41)$$

with $H_N(r)$ is a known nonlinear function.

Let ψ_d be the desired output of the system.

Step 1 : We define the error variable $e_1 = \psi - \psi_d$. Its derivative gives:

$$\dot{e}_1 = \dot{\psi} - \dot{\psi}_d = r - \dot{\psi}_d \quad (42)$$

Consider the following Lyapunov control function:

$$V_1 = \frac{1}{2} e_1^2 \quad (43)$$

Its derivative then gives:

$$\dot{V}_1 = e_1 \dot{e}_1 \quad (44)$$

So

$$\dot{V}_1 = e_1 (r - \dot{\psi}_d) \quad (45)$$

To ensure the convergence of e_1 , the derivative of the Lyapunov control function must be defined negative therefore,

$$r - \dot{\psi}_d = -k_1 e_1 - \beta_1 \tanh(\alpha_1 e_1) \quad (46)$$

with $\beta_1 > 0$ et $\alpha_1 > 0$

So,

$$r_d = -k_1 e_1 - \beta_1 \tanh(\alpha_1 e_1) + \dot{\psi}_d \quad (47)$$

And

$$\dot{V}_1 = -k_1 e_1^2 - \beta_1 e_1 \tanh(\alpha_1 e_1) \quad (48)$$

Step 2 : We define the error variable $e_2 = r - r_d$. Its derivative gives:

$$\dot{e}_2 = \dot{r} - \dot{r}_d = -\frac{H_N(r)}{T} + \frac{K}{T} \delta + \frac{w(t, \psi, r)\Delta}{T} - \dot{r}_d \quad (49)$$

The nonlinear function $-\frac{H_N(r)}{T}$ composing the model is sometimes difficult to implement in practice. With its approximation by an artificial neural network $\theta^T \xi(r)$, equation (49) gives:

$$\dot{e}_2 = \theta^T \xi(r) + \frac{K}{T} \delta + \frac{w(t, \psi, r) \Delta}{T} - \dot{r}_d \quad (50)$$

Consider the following Lyapunov control function:

$$V_2 = V_1 + \frac{1}{2} e_2^2 \quad (51)$$

Its derivative gives:

$$\dot{V}_2 = -k_1 e_1^2 - \beta_1 e_1 \tanh(\alpha_1 e_1) + e_2 \dot{e}_2 \quad (52)$$

So

$$\dot{V}_2 = -k_1 e_1^2 - \beta_1 e_1 \tanh(\alpha_1 e_1) + e_2 (\theta^T \xi(r) + \frac{w(t, \psi, r) \Delta}{T} - \dot{r}_d) \quad (53)$$

The method of nonlinear damping makes it possible to calculate the command which ensures bounded trajectories of (41), despite the presence of uncertainties, therefore:

$$\delta = \alpha_1 + \varsigma \quad (54)$$

So, equation (53) gives:

$$\dot{V}_2 = -k_1 e_1^2 - \beta_1 e_1 \tanh(\alpha_1 e_1) - k_2 e_2^2 - \beta_2 e_2 \tanh(\alpha_2 e_2) + e_2 (\frac{K}{T} \varsigma + \frac{w(t, \psi, r) \Delta}{T}) \quad (55)$$

because the nominal command of the rudder angle is given by equation (37).

With

$$\varsigma = -m_1 e_2 w^2 \quad (56)$$

where $m_1 > 0$ is a design parameter.

So, equation (55) then becomes :

$$\dot{V}_2 = -k_1 e_1^2 - \beta_1 e_1 \tanh(\alpha_1 e_1) - k_2 e_2^2 - \beta_2 e_2 \tanh(\alpha_2 e_2) - \frac{K m_1 e_2^2 w^2}{T} + \frac{e_2 w \Delta}{T} \quad (57)$$

where

$$-\frac{K m_1 e_2^2 w^2}{T} + \frac{w \Delta e_2}{T} = -\frac{K m_1}{T} \left[e_2 w - \frac{\Delta}{2 K m_1} \right]^2 + \frac{\Delta^2}{4 K T m_1}$$

Since Δ is bounded by Δ_0 and $K T > 1$, then

$$\dot{V}_2 \leq -k_1 e_1^2 - \beta_1 e_1 \tanh(\alpha_1 e_1) - k_2 e_2^2 - \beta_2 e_2 \tanh(\alpha_2 e_2) + \frac{\Delta_0^2}{4 m_1} \quad (58)$$

This result implies that \dot{V}_2 is negative outside a certain plane, and that e_1 and e_2 are bounded (the bound depends on Δ_0 and m_1), despite the presence of uncertainties.

5. Simulation

Assumption 1:

- The known nonlinear term w composing the external disturbance is a ramp function with slope equal to 2
- The uncertain nonlinear term is bounded by $\Delta_0 = 4$ so $|\Delta| < 4$
- The operating speed of the cargo ship is constant

5.1. Course-keeping maneuver

5.1.1. Nominal backstepping control

Figure 5 shows the result in course-keeping maneuver simulation of the nominal nonlinear autopiloting cargo ship with the rudder control law defined by equation (32). The nominal nonlinear system has great accuracy because in steady state the difference between the reference ψ_d and the output ψ is zero as shown in figure 6. The system is also very fast because the rise time, which is defined as the time taken for the system to reach 90% of the final value, is approximately 0.2s. However, it shows a very slight overshoot at the reference jump point.

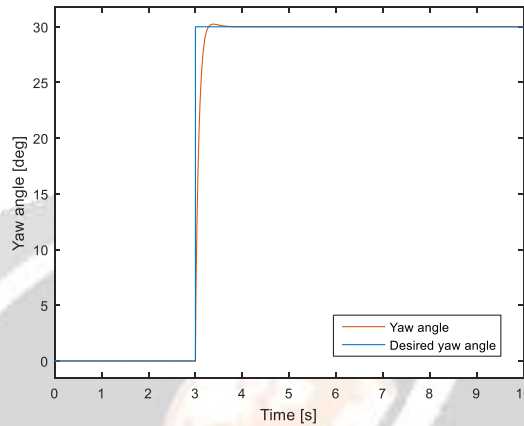


Figure 5 : Nominal system response in course-keeping

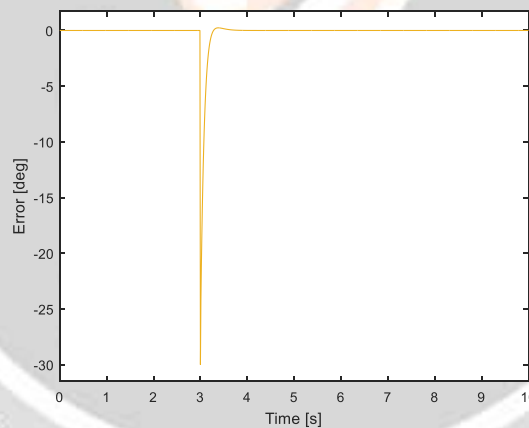


Figure 6 : Error signal of the nominal system in course-keeping

The rudder angle δ is given in figure 7. In steady state and before the jump at $t = 3s$, we see that the rudder angle has a constant value of 633.6 deg . In addition, an alternative pulse can be seen at the reference jump point. This is due to the sudden variation of the reference which has an infinite tangent at time $t = 3s$.

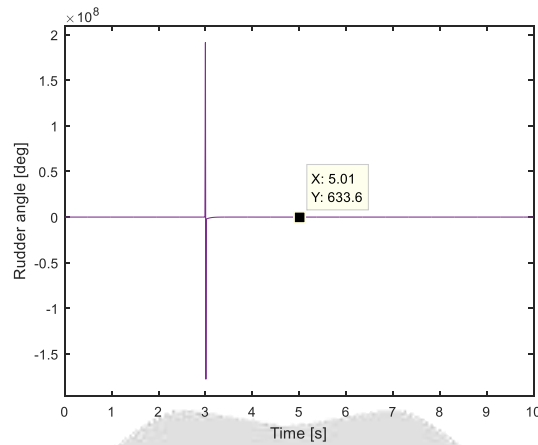


Figure 7 : Rudder angle δ

5.1.2. « Efficient » nominal backstepping control

Figure 8 shows the result in course-keeping maneuver simulation of the « efficient » nominal nonlinear autopiloting cargo ship with the rudder control law defined by equation (37). The « efficient » nominal nonlinear system has great accuracy because in steady state the difference between the reference ψ_d and the output ψ is zero as shown in **figure 9**. The system is also very fast because the rise time, which is defined as the time taken for the system to reach 90% of the final value, is approximately 0.1s.

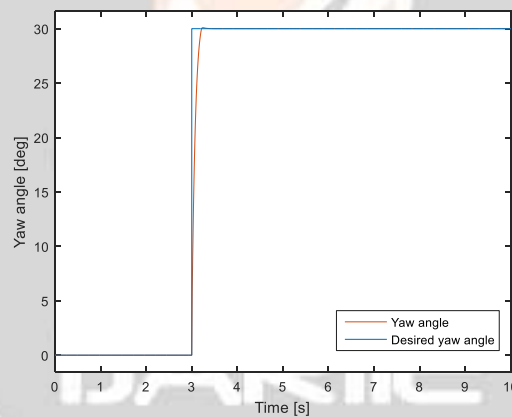


Figure 8 : Efficient nominal system response in course-keeping

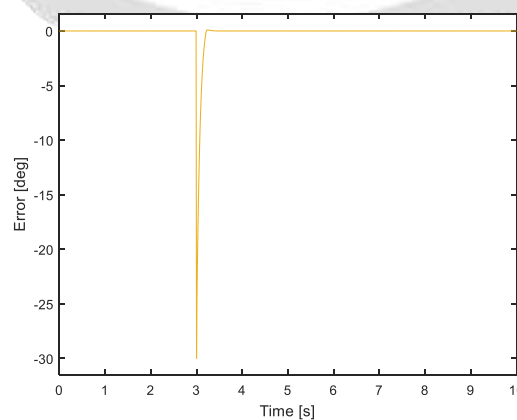


Figure 9 : Efficient nominal error signal in course-keeping

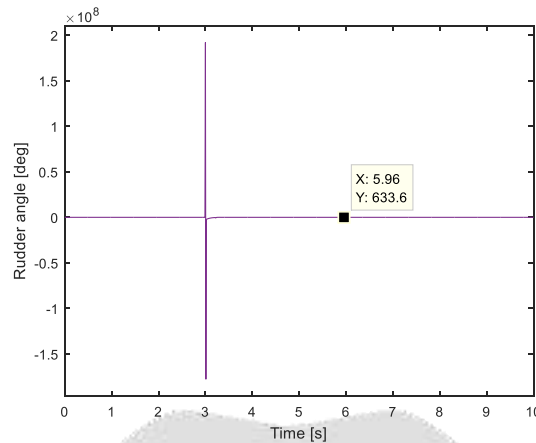


Figure 10 : Rudder angle δ

The rudder angle δ is given in **figure 10**. In steady state and before the jump at $t = 3s$, we see that the rudder angle has a constant value of 633.6 deg . In addition, an alternative pulse can be seen at the reference jump point. This is due to the sudden variation of the reference which has an infinite tangent at time $t = 3s$.

Remark 3:

We notice an increase in the performance of the nominal system in course-keeping with the use of the performance term $\tanh ()$ because:

- there is disappearance of the overshoot
- the rise time has gone from $0.2s$ to $0.1s$

5.1.3. Robust backstepping control

Figure 11 shows the result in course-keeping maneuver simulation of the robust nonlinear autopiloting cargo ship with the rudder control law defined by equation (54). The robust nonlinear system has great accuracy because in steady state the difference between the reference ψ_d and the output ψ is zero as shown in **figure 12**. The system is also very fast because the rise time, which is defined as the time taken for the system to reach 90% of the final value, is approximately $0.1s$.

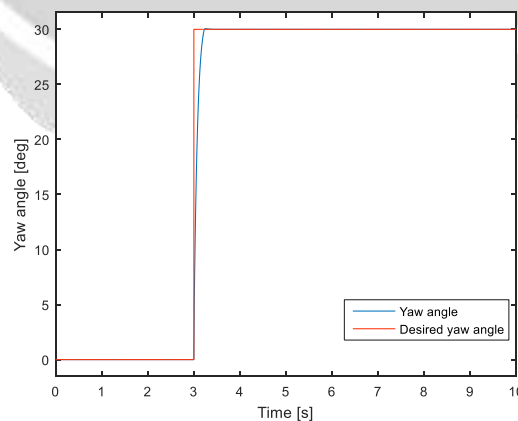


Figure 11 : Robust system response in course-keeping

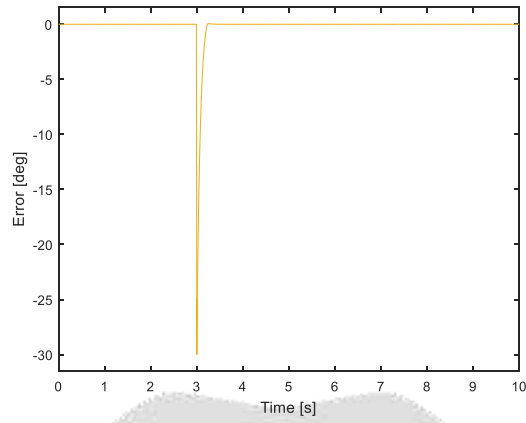


Figure 12 : Error signal of the robust system in course-keeping

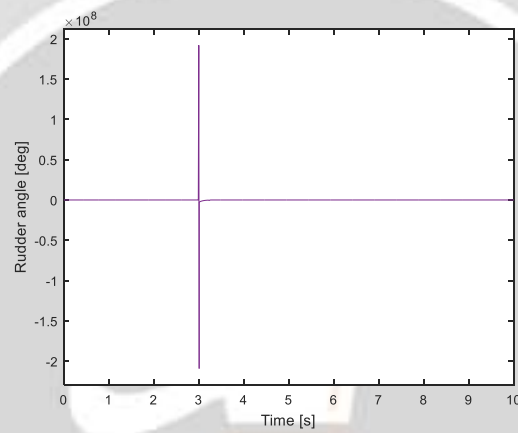


Figure 13 : Rudder angle δ for $t \in [0,10]$

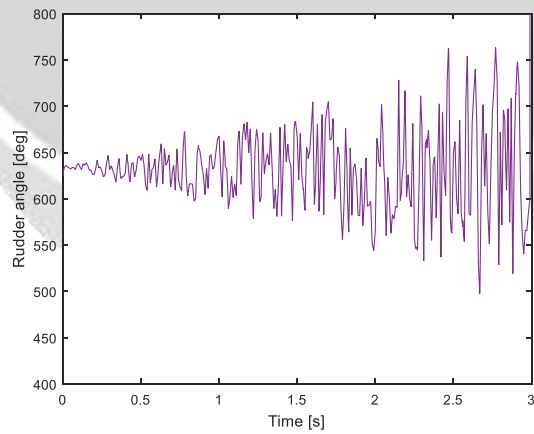


Figure 14 : Rudder angle δ pour $t \in [0,3]$

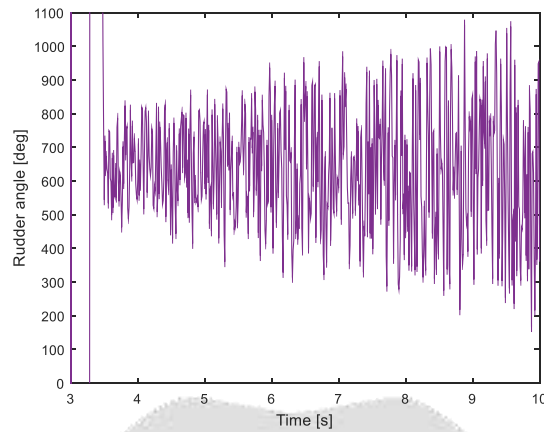


Figure 15 : Rudder angle δ pour $t \in [3,10]$

The rudder angle δ is given by figures 13, 14 and 15. At the jump point $t = 3s$, the rudder angle presents an alternative pulse as shown in figure 13. This is due to the sudden variation of the reference which has an infinite tangent at time $t = 3s$. Before the jump, the rudder angle is given by figure 14. And after the jump, figure 15 shows us the evolution of the rudder angle.

Remark 4:

It can be seen that the external disturbance is rejected by the robust system in course-keeping.

5.2. Turning maneuver

5.2.1. Nominal backstepping control

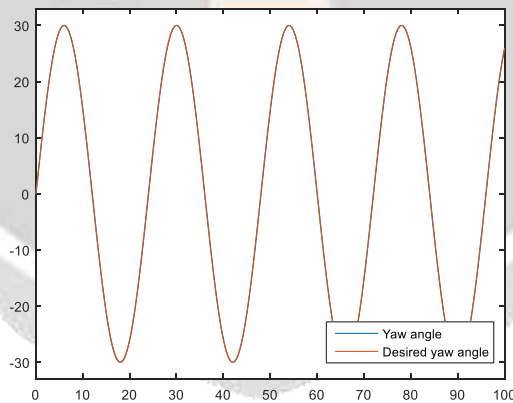


Figure 16 : Nominal system response to a sine wave input

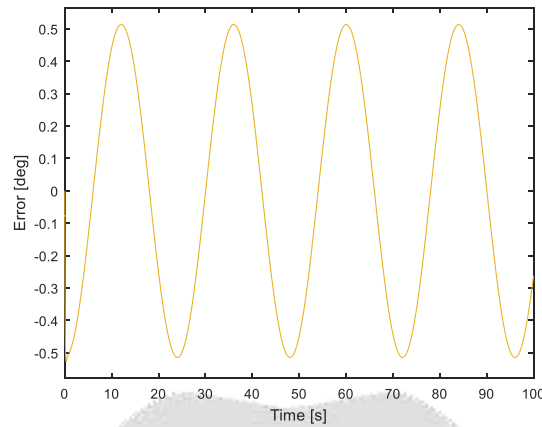


Figure 17 : Error signal of the nominal system to a sine wave input

Figure 16 shows the results in turning maneuver simulation of the nominal nonlinear autopiloting cargo ship with the rudder control law defined by equation (32). We can see that the output of the nominal system follows the sinusoidal reference very well. The difference between the reference ψ_d and the yaw angle ψ is sinusoidal with the same frequency as the reference and amplitude close to 0.51 deg as shown in **figure 17**.

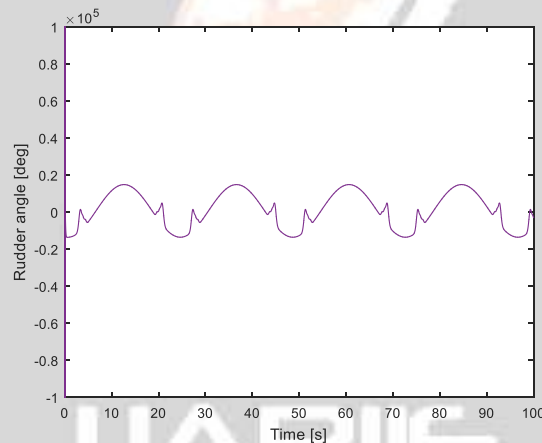


Figure 18 : Rudder angle δ

The rudder angle δ is given in **figure 18**. It is periodic with a maximum value close to 1.5×10^4 deg and the same frequency as the reference equal to 15 deg/s.

5.2.2. « Efficient » nominal backstepping control

Figure 19 shows the results in turning maneuver simulation of the « efficient » nominal nonlinear autopiloting cargo ship with the rudder control law defined by equation (37). We can see that the output of the « efficient » nominal system follows the sinusoidal reference very well. The difference between the reference ψ_d and the yaw angle ψ is sinusoidal with the same frequency as the reference and amplitude close to 0.15 deg as shown in **figure 20**.

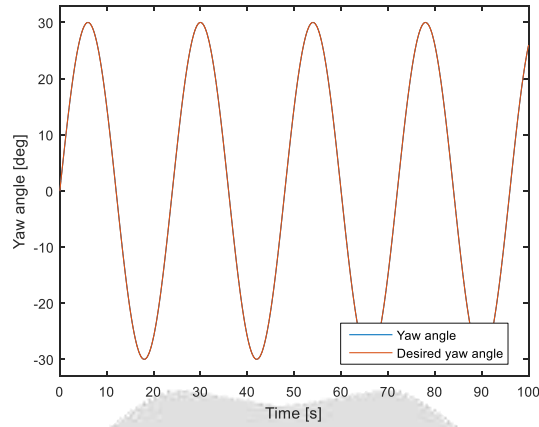


Figure 19 : « Efficient » nominal system response to a sine wave input

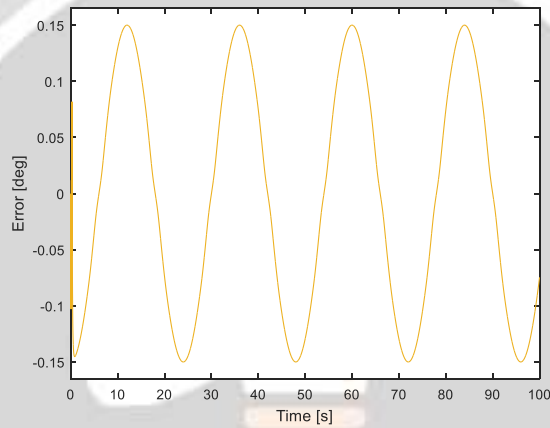


Figure 20 : Error signal of the « efficient » nominal system to a sine wave input

The rudder angle δ is given in **figure 21**. It is periodic with a maximum value close to 1.9×10^4 deg and the same frequency as the reference equal to 15 deg/s.

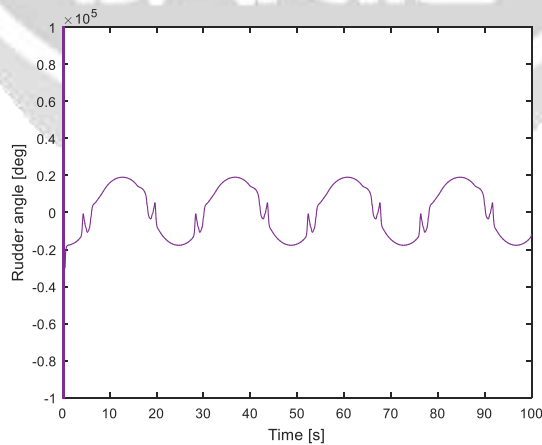


Figure 21 : Rudder angle δ

Remark 5 :

We notice an increase in the performance of the nominal system in turning maneuver because the difference between the reference ψ_d and the yaw angle ψ has gone from 0.51 deg to 0.15 deg.

5.2.3. Robust backstepping control

Figure 22 shows the results in turning maneuver simulation of the robust nonlinear autopiloting cargo ship with the rudder control law defined by equation (54). We can see that the output of the robust system follows the sinusoidal reference very well despite the uncertain environmental disturbance. The difference between the reference ψ_d and the yaw angle ψ is given in **figure 23** with a maximum value of 0.18deg.

The rudder angle δ is given in **figure 24**. It has several positive and negative pulses.

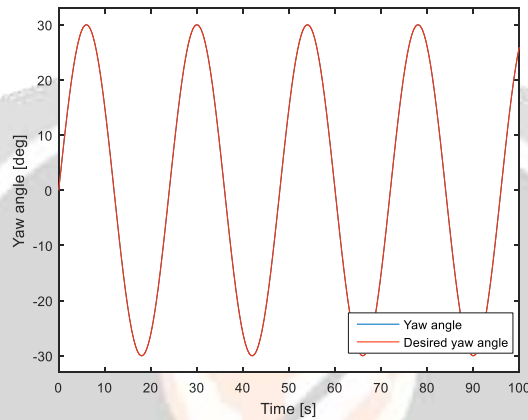


Figure 22 : Robust system response to a sine wave input

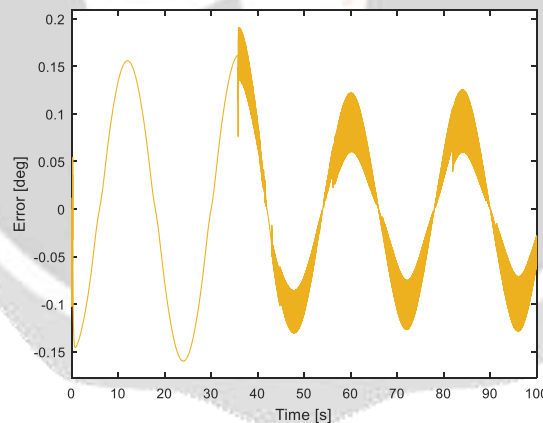


Figure 23 : Error signal of the robust system to a sine wave input

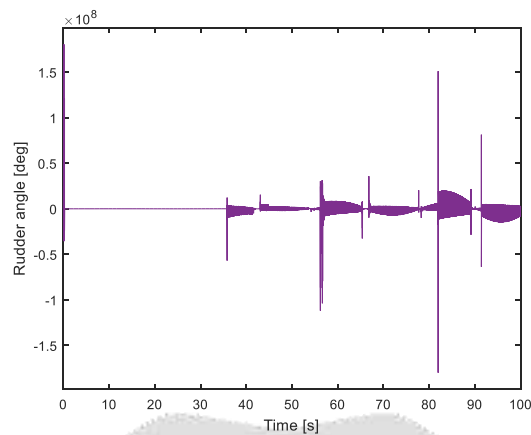


Figure 24 : Rudder angle δ

6. Conclusion

The synthesis of robust autopilot guarantees high performance in autopiloting of a cargo ship. It makes it possible to cancel the influence of external disturbance to the system and to ensure the cargo ship's maneuvering function while course-keeping and turning.

7. References

- [1] www.wikipedia.org/wiki/Freighter, 15 October 2020
- [2] K. Nomoto, T. Taguchi, K. Honda, S. Hirano, « *On the steering qualities of ships* », International Shipbuilding Progress, 1957
- [3] N.H.Noorbin, « *On the design and analyse of the zig zag test on base of quasi linear frequency response* », Suede, 1963
- [4] M.I.Bech et S.Wagner, « *Analogue simulation of ship maneuvers* », hydro and aerodynamics laboratory, Danemark, 1969
- [5] M. Kritic, I. Kanellakopoulos, P. V. kokotovic, « *Nonlinear and Adaptative Control Design* », New York, 1995
- [6] I. Kanellakopoulos, P. V. Kokotovic, A. S. Morse, « *Systematic design of adaptive controller for feedback linearizable systems* », IEEE, 1991.
- [7] R. R. Rasoamanana, P.A. Randriamitsoa, A.A. Randriamitsoa, « *Synthèse d'une loi de commande non linéaire par la méthode backstepping intégrateur d'un système de suspension hydraulique d'un véhicule* », Mada-ETI, 2017
- [8] Y. Li, S. Qiang, X. Zhuang, O. Kaynak, « *Robust and adaptive backstepping control for nonlinear systems using RBF neural network* », IEEE, 2004